

This accepted version of an article published by online by Elsevier on 25 April 2017 in *Agricultural Systems*. Published version available from: <https://doi.org/10.1016/j.agsy.2017.04.006>

Accepted version made available under [CC-BY-NC-ND 4.0 International License](https://creativecommons.org/licenses/by-nc-nd/4.0/) from SOAS Research Online:

<http://eprints.soas.ac.uk/24041/>

1
2 **Maintaining Rice Production while Mitigating Methane and Nitrous Oxide**
3 **Emissions from Paddy Fields in China:**
4 **Evaluating Tradeoffs by Using Coupled Agricultural Systems Models**

5
6 Zhan Tian¹, Yilong Niu^{1,2}, Dongli Fan², Laixiang Sun^{3,4,5}, Gunther Ficsher⁴, Honglin Zhong³,
7 Jia Deng⁶, Francesco N. Tubiello⁷

- 8
9
10 1. Shanghai Climate Center, Shanghai Key Laboratory of Meteorology and Health,
11 Shanghai Meteorological Service, Shanghai 200030, China
12 2. Shanghai Institute of Technology, Shanghai, 201418
13 3. Department of Geographical Sciences, University of Maryland, College Park, MD 20742,
14 USA
15 4. International Institute for Applied Systems Analysis (IIASA), A-2361 Laxenburg, Austria
16 5. School of Finance & Management, SOAS, University of London, London WC1H 0XG,
17 UK
18 6. Earth Systems Research Center, Institute for the Study of Earth, Oceans, and Space,
19 University of New Hampshire Durham, NH 03824, USA
20 7. Statistics Division, Food and Agriculture Organization of the United Nations (FAO),
21 Rome, Italy

22
23
24
25
26 **Correspondence to:** Dongli FAN, E-mail: fandl@sit.edu.cn; or Laixiang Sun, Email:

27 LSun123@umd.edu, Tel: +1-301-405-8131, Fax: +1-301-314-9299.

28
29
30
31
32
33 **Acknowledgement:**

34 This work was supported by the National Natural Science Foundation of China (Grant Nos.
35 41601049, 41371110, and 41671113) and the National Key Research and Development
36 Program of China (Grant No. 2016YFC0502702).

37

39 **ABSTRACT**

40
41 China is the largest rice producing and consuming country in the world, accounting for more
42 than 25% of global production and consumption. Rice cultivation is also one of the main
43 sources of anthropogenic methane (CH₄) and nitrous oxide (N₂O) emissions. The challenge
44 of maintaining food security while reducing greenhouse gas emissions is an important
45 tradeoff issue for both scientists and policy makers. A systematical evaluation of tradeoffs
46 requires attention across spatial scales and over time in order to characterize the complex
47 interactions across agricultural systems components. We couple three well-known models
48 that capture different key agricultural processes in order to improve the tradeoff analysis.
49 These models are the DNDC biogeochemical model of soil denitrification-decomposition
50 processes, the DSSAT crop growth and development model for decision support and agro-
51 technology analysis, and the regional AEZ crop productivity assessment tool based on agro-
52 ecological analysis. The calibration of eco-physiological parameters and model evaluation
53 used the phenology and management records of 1981-2010 at nine agro-meteorological
54 stations spanning the major rice producing regions of China. The eco-physiological
55 parameters were calibrated with the GLUE optimization algorithms of DSSAT and then
56 converted to the counterparts of DNDC. The upscaling of DNDC was carried out within each
57 cropping zone as classified by AEZ. The emissions of CH₄ and N₂O associated with rice
58 production under different management scenarios were simulated with the DNDC at each site
59 and also each 10×10 km grid-cell across each cropping zone. Our results indicate that it is
60 feasible to maintain rice yields while reducing CH₄ and N₂O emissions through careful
61 management changes. Our simulations indicated that a reduction of fertilizer applications by
62 5-35% and the introduction of midseason drainage across the nine study sites resulted in
63 reduced CH₄ emission by 17-40% and N₂O emission by 12-60%, without negative
64 consequences on rice yield.

65
66 **KEY WORDS:** Climate change; agricultural CH₄ and N₂O emissions; rice yield; model
67 coupling; mitigation tradeoffs; China

68

69 **INTRODUCTION**

70 Climate change characterized by global warming has already had observable impact on
71 the ecological system and human society (Alley et al., 2003). The historical records show that
72 from 1901 to 2012, the global mean surface temperature increased by 0.89°C. This warming
73 trend is expected to continue in the forthcoming decades and would impose even more
74 significant impact on ecosystem and human society (IPCC, 2013). The main cause of current
75 global warming is the anthropogenic emission of greenhouse gases (GHGs), which has led to
76 their increased concentration in the atmosphere. Modern intensive farming, which heavily
77 depends on chemical fertilizer application and irrigation, is the single largest source of
78 methane (CH₄) and nitrous oxide (N₂O) emissions (IPCC, 2014; FAO, 2016). Meanwhile, a
79 warmer climate accompanied by modified water regimes exerts impact on farming practices
80 and consequently on crop productivity (Verburg et al., 2000; IPCC, 2014). Since the global
81 warming potential of CH₄ and N₂O is 25 and 298 times higher than CO₂, respectively (IPCC,
82 2013), it is well recognized that a focus on reducing CH₄ or N₂O emissions may be an
83 effective climate change mitigation strategy.

84 Our ability to pick these “low-hanging fruits” may however be constrained by the
85 existence of multiple, conflicting objectives. Rice paddy cultivation in China represents a
86 significant example to this end. On the one hand, China is the major producer and consumer
87 of rice in the world and maintaining self-sufficiency in rice is extremely important for the
88 country (FAOSTAT 2016). On the other, China’s rice production generates significant
89 environmental pressure, as it depends on large-scale basin irrigation and large amounts of
90 fertilizers applications (Miao et al., 2011). Such practices have resulted in significant
91 emissions of CH₄ and N₂O to the atmosphere, as well as damages to soil and water systems.
92 Using IPCC guidelines for GHG inventories (IPCC, 2006), the emissions of CH₄ from
93 Chinese paddy fields were estimated at 7.41 Tg (1 Tg = 10¹² g) CH₄-C in 2000, which is well
94 over 150 Tg CO₂eq, accounting for about 29% of world total CH₄ emission from rice in that
95 year (Yan et al., 2009). These emissions levels were maintained throughout the last decade
96 (FAOSTAT, 2016). At the same time, N₂O emissions from Chinese paddy fields were
97 estimated at 0.036 Tg N₂O-N in 2007 (Gao et al. 2011), corresponding to roughly 30% of the
98 total N₂O-N emissions from Chinese agriculture (FAOSTAT, 2016).

99 In the rice cultivation system, rice grain and greenhouse gas are joint products from
100 paddy fields cultivation and there is a complex relationship between rice growing and GHG
101 emissions. For example, CH₄ production is influenced by substrate concentrations, which are

102 influenced by plant root activities. Plant growth dynamic also influences soil mineral N
103 through crop N uptake, therefore indirectly affecting N₂O emission. This complexity has
104 attracted significant research attention and various GHG mitigation measures have been
105 tested using field experiments at paddy sites. For example, Dong et al. (2011) highlighted the
106 tradeoff relationship between CH₄ and N₂O emissions, finding that an increasing application
107 of nitrogen fertilizer will mitigate CH₄ emission with reference to no fertilization, but
108 increase N₂O emissions at the same time. Itoh et al. (2011) found that employing midseason
109 drainage as a water management technique in rice fields reduced the combined climate
110 forcing of CH₄ and N₂O in comparison with basin irrigation. Based on experimental evidence,
111 Johnson-Beebout et al. (2009) concluded that simultaneous minimization of both CH₄ and
112 N₂O emission could not be maintained in rice soils, but that appropriate water and residue
113 management could nonetheless reduce greenhouse gas emissions. Wu et al. (2008) showed
114 that employing conservation tillage methods, especially no-tillage, mitigated GHG emission
115 from rice fields by about 15%. However, it is difficult to extrapolate these field-based results
116 to large regional scales, because of high inherent variability over space and time. Such
117 variability may instead be addressed by agricultural systems models that, while capturing the
118 fundamental soil crop atmosphere dynamics highlighted by field experiments, can be used to
119 further estimate the regional variability of associated emissions as a function of the wide
120 range of soil, water and climatic parameters that exists over large scales (Jones et al., 2016).

121 The DeNitrification-DeComposition (DNDC) model is one of the most widely accepted
122 biogeochemistry process-based models in the world (Wang and Chen, 2012; Gilhespy et al.,
123 2014). The model has been evaluated against observations worldwide (e.g., Beheydt et al.,
124 2007; Giltrap et al., 2010; Gilhespy et al., 2014). The development of a GIS coupled to high-
125 resolution soil maps in recent versions of this model, allows DNDC to also estimate GHG
126 emissions at regional and national levels, in support of national inventories and including the
127 impacts of rice rotations (e.g., Gilhespy et al., 2014; Zhang et al. 2016; Li et al. 2005; Chen et
128 al. 2016).

129 With the GIS application, an array of weather and soil data could be employed to
130 support DNDC model-based regional simulations. However, two limitations currently
131 undermine such simulations. First, the phenological and physiological parameters as the key
132 input of DNDC are typically calibrated with the subjective optimization method (McCuen,
133 2003), meaning that parameter values are manually adjusted based on the modeler's
134 subjective knowledge of the parameter, model, and data (Wang and Chen, 2012). A
135 consequence of this limitation is that the default cultivar parameter values in DNDC

136 characterize only one rice cultivar for all of China, thus failing to represent the richness and
137 regional diversity of cultivars that exists in this country. Second, as highlighted in Zhang et al.
138 (2016), most DNDC studies were conducted at the county level in the case of China or at
139 large spatial simulation units, with a resolution about $0.5^{\circ} \times 0.5^{\circ}$ (e.g., Li, 2000; Pathak et al.,
140 2005; Tang et al., 2006; Gao et al., 2014). This coarseness does not allow to properly capture
141 the impacts of soil heterogeneity and the associated management measures within a county or
142 a large spatial unit, resulting in poor spatial performance of the simulation models.

143 To overcome the above weaknesses of DNDC and to more accurately evaluate the
144 tradeoffs between maintaining the current level of rice production and reducing GHG
145 emissions from farming activities, we coupled three state-of-the-art agricultural systems
146 models in order to capitalize on their individual comparative advantages. They are the
147 biogeochemistry process-focused DNDC model, the crop growing process-focused model –
148 Decision Support System for Agro-technology Transfer (DSSAT) (Jones et al. 2003), and the
149 Agro-Ecological Zone (AEZ) model (Fischer et al. 2012), a widely used regional crop
150 productivity assessment tool. The two crop simulation models (DSSAT and AEZ) are
151 designed to assess the impacts of multiple climate factors on crop growth and grain yield.
152 They are widely employed in climate impact studies (Challinor et al., 2014; Thorp et al.,
153 2008; Seidl et al., 2001). We investigated how such coupling can improve the spatial
154 performance of DNDC for the case of paddy rice production in China. Our parameters
155 calibration and model evaluation used the observed phenology and management records at
156 nine representative agro-meteorological stations, spanning the major rice producing regions
157 of China. We first calibrated eco-physiological (cultivar) parameters for rice growth using the
158 Generalized Likelihood Uncertainty Estimation (GLUE) algorithm provided by DSSAT,
159 which uses Monte Carlo sampling from prior distributions of the coefficients and a Gaussian
160 likelihood function to determine the best cultivar coefficients, based on the observation data.
161 We then followed a procedure as presented in Section 2.4.2 to convert these eco-
162 physiological cultivar parameters into DNDC required parameters. In this way, we enriched
163 the value set of cultivar parameters of the DNDC model, which is essential for meaningfully
164 upscaling, via the assistance of AEZ, the DNDC runs to the rice cropping zones of China.
165 With such coupling between the three models, we evaluated rice yield levels and the
166 corresponding CH_4 and N_2O emissions under different management scenarios, at a resolution
167 of 10×10 km, seeking to highlight those water and fertilizer management solutions that could
168 lead to significant reduction of CH_4 and N_2O emissions without causing reductions in rice

169 production.

170

171 **2. MATERIALS AND METHODS**

172 **2.1 The study sites**

173 We selected nine agro-meteorological observation stations based on the following
174 criteria from the original hardcopy records filed in the Data Center of China Meteorological
175 Administration: (1) each station represents a typical cropping system for rice cultivation in
176 China; (2) they differ in terms of geographic and climatologic characteristics; (3) each station
177 has complete records of crop phenology for more than 20 years over the period of 1981-2010;
178 and (4) each station has complete records of crop management for more than 5 years over the
179 period of 1981-2010. These records include the ID, name and location (latitude and longitude)
180 of each station; date of each major phenological stages (sowing, flowering, maturity, etc.);
181 yield and yield components (grain weight, grain number per tiller, tiller number per plant,
182 etc.); date, type and quantity of fertilizer application; and irrigation methods and dates. These
183 crop phenology and management data are critical for simulating crop growing and
184 quantifying CH₄ and N₂O emission from crop fields. Table 1 and Figure 1 report names,
185 locations, and geographical features of these nine stations.

186

187 *(Table 1 and Figure 1 are about here)*

188

189 **2.2 Input Datasets at the Grid-cell Level**

190 Observed daily weather data, including minimum and maximum air temperature, daily
191 sunshine hours, precipitation, relative humidity, and wind speed, for 1981-2010 at over 700
192 observation stations nationwide were provided by the Data Center of China Meteorological
193 Administration. Because all three models need solar radiation data, we employed the
194 empirical global radiation model to calculate daily radiation levels (Pohlert, 2004). These
195 point-based data are imported to ArcGIS together with the coordinates and then interpolated
196 into 10 km spatial resolution raster data.

197 The Harmonized World Soil Database (HWSD, cf. FAO/IIASA/ISRIC/ISSCAS/JRC,
198 2009) provides reliable and harmonized soil information at the grid cell level for the world,
199 with a spatial resolution of 1 km × 1 km for China. The soil is divided into topsoil (0–30 cm)
200 and subsoil (30–100 cm). Each grid cell in the database is linked to commonly used soil
201 parameters. Most of the minimum soil properties required by the DSSAT and DNDC models
202 can be extracted directly from the HWSD soil database. For the missing soil surface albedo,

203 we used the soil color from the World Inventory of Soil Emission Potentials (WISE) soil
204 database (Batjes, 2009) and determined the soil surface albedo with the standard given by
205 Ritchie et al. (1989). We calculated other missing soil properties with extracted soil properties
206 and procedures provided in the DSSAT literature (Gijssman et al., 2002, 2007), such as USDA
207 curve number (Lane, 1982) and drainage rate, root growth factor, upper and lower limit of
208 plant extractable soil water.

209 The map of paddy fields is extracted from the National Land Cover database (100 m ×
210 100 m) provided by the Institute of Geographical Sciences and Natural Resource Research
211 (IGSNRR) of the Chinese Academy of Sciences. The reference year for the map is 2000. This
212 land cover database is produced from visual interpretation of Landsat ETM/ETM+ satellite
213 images and grouped into ten categories. Paddy field is one of the major categories (Liu et al.,
214 2005).

215

216 **2.3 Agricultural Systems Models**

217 **2.3.1 The DNDC model**

218 The DeNitrification-DeComposition (DNDC) model simulates soil carbon (C) and
219 nitrogen (N) biogeochemical processes in crop growth cycle. It was originally developed for
220 simulating C sequestration and emissions of greenhouse gases from agricultural soils in the
221 USA (Li et al., 1992; Li et al., 1994). During the last 25 years, the DNDC model has been
222 developed to simulate C and N transformations in different ecosystems, such as forest,
223 wetlands, pasture, and livestock farms. It has incorporated a relatively complete suite of
224 biophysical and biogeochemical processes, which enables it to compute the complex
225 transport and transformations of C and N in terrestrial ecosystems under both aerobic and
226 anaerobic conditions (Gilhespy et al., 2014; Li 2007).

227 DNDC is comprised of six interacting sub-models: soil climate, plant growth,
228 decomposition, nitrification, denitrification, and fermentation. The soil climate, plant growth,
229 and decomposition sub-models convert the primary drivers into soil environmental factors.
230 The nitrification, denitrification, and fermentation sub-models simulate C and N
231 transformations that are mediated by soil microbes and controlled by soil environmental
232 factors (Li 2000; Li et al., 2012). In DNDC, crop biomass and yield are simulated at daily
233 time steps by considering the effects of several environmental factors on plant growth,
234 including radiation, air temperature, soil moisture, and N availability. Methane flux is
235 predicted by modeling CH₄ production, oxidation, and transport processes. CH₄ production is
236 simulated by calculating substrate concentrations (i.e., electron donors and acceptors)

237 resulting from decomposition of SOC (soil organic carbon) as well as plant root activities
238 including exudation and respiration, and then by simulating a series of reductive reactions
239 between electron donors (i.e., H₂ and dissolved organic carbon) and acceptors (i.e., NO₃⁻,
240 Mn⁴⁺, Fe³⁺, SO₄²⁻, and CO₂). Redox potential, temperature, pH, along with the concentrations
241 of electron donors and acceptors are the major factors controlling the rates of CH₄ production
242 and oxidation. DNDC simulates CH₄ transport via three pathways, including plant-mediated
243 transport, ebullition, and diffusion (Fumoto et al., 2008; Zhang et al., 2002). N₂O is simulated
244 as a by-product of nitrification and denitrification. As microbial-mediated processes, both
245 nitrification and denitrification are subject to complex regulation of numerous environmental
246 factors, such as concentrations of mineral N, availability of dissolvable organic carbon
247 (DOC), redox potential, and temperature in DNDC (Li, 2000). Farming management
248 practices, such as synthetic fertilizer application, manure use and irrigation, have been
249 parameterized to regulate the soil N dynamics, DOC availability, and/or soil environments,
250 and therefore regulate N₂O emissions from soils. In this research, we use the latest version of
251 DNDC (DNDC 95).

252

253 **2.3.2 The DSSAT model**

254 The Decision Support System for Agro-technology Transfer (DSSAT) model (Jones et
255 al., 2003; Hoogenboom et al. 2010) is a popularly-employed model for simulating crop
256 growing dynamics (Challinor et al., 2014). The core of the DSSAT system consists of 17 crop
257 simulation models. This research employs the Crop Environment Resource Synthesis
258 (CERES) model, which simulates cereal crops such as wheat, rice and maize. The CERES
259 model calculates daily phenological development (i.e., vegetative growth, flowering, grain
260 growth, maturity and senescence phases) and biomass production in response to
261 environmental (soil and climate) and management (crop variety, planting conditions, N
262 fertilization, and irrigation) factors.

263 The crop cultivar parameters, which are named genetic coefficients in DSSAT,
264 quantitatively describe how a particular genotype of a cultivar responds to environmental
265 factors (Penning de Vries et al., 1992), thus enabling the integration of genetic information on
266 physiological traits into crop growth models. Each crop in the model has a specific set of
267 parameters, values of which characterizes the genetic information of different cultivars. In the
268 CERES-rice model, 8 parameters are essential for describing the genetic information of
269 different rice cultivars (Prasada Rao, 2008, Table 14.1). Because each station belongs to a
270 specific cropping zone/cropping system for rice cultivation in China as we presented in

271 Section 2.1, we have nine cultivars, each at one station. We employ the DSSAT-provided
272 Generalized Likelihood Uncertainty Estimation (GLUE) method (He et al., 2010) to estimate
273 the parameter values of the given cultivar. GLUE is a Bayesian estimation method. GLUE
274 uses Monte Carlo sampling from prior distributions of the coefficients and a Gaussian
275 likelihood function to determine the best coefficients based on the observation data. It has
276 been widely used in crop and hydrological modeling (Blasone et al. 2008; He et al., 2010;
277 Wang et al. 2015). The technical details of the GLUE estimation and a part of the estimation
278 results were published in Tian et al. (2014). The procedure on translating DSSAT's genetic
279 coefficients into the format of DNDC's cultivar parameters will be presented in sub-section
280 2.4.2.

281 282 **2.3.3 The AEZ model**

283 In contrast to the process-based crop growth model like DSSAT, the Agro-Ecological
284 Zone (AEZ) model, which was jointly developed by the International Institute for Applied
285 Systems Analysis (IIASA) and the Food and Agricultural Organization (FAO) of the United
286 Nations, is a regional scale model to simulate land resource and crop production potential
287 (Fischer et al., 2012). AEZ provides a standardized crop-modeling and environmental
288 matching procedure, which classify a region into cropping zones based on climate, soil, and
289 terrain characteristics relevant to specific crop production, and identify crop-specific
290 limitations of prevailing agro-ecological resources under assumed levels of inputs and
291 management conditions. This procedure in AEZ makes it well suited for crop suitability,
292 zoning, and productivity assessments at regional, national and global scales (cf., among
293 others, FAO, 2007; Fischer et al., 2005; Gohari et al., 2013; Masutomi et al., 2009; Tian et al.,
294 2012, 2014; Tubiello and Fischer, 2007). In each rice-cropping zone identified by the AEZ,
295 we have one representative observation station (Fig. 1). We assume that the rice cultivar
296 parameters we have calibrated at the representative station are applicable for DNDC
297 simulations across grid cells within this rice cropping zone.

298 299 **2.4 Implementation Procedure of Model Coupling**

300 The flowchart for effectively linking DSSAT, AEZ, and DNDC models are presented in
301 Fig. 2. As shown in Fig.2, the central purpose of the model coupling is for finding feasible
302 ways to reconcile the two policy goals of maintaining rice production and mitigating methane
303 (CH_4) and nitrous oxide (N_2O) emissions from paddy fields in China. The reconciliation
304 would become more convincing if both rice production and the corresponding CH_4 and N_2O

emissions are outputs of one model, and the most suitable model for this purpose is the DNDC. However, despite that DNDC model has the designed comparative advantage in simulating biogeochemistry process during crop growing cycle and it is also capable of simulating crop growing process, its simulations are subject to the condition that the representative phenological and physiological parameters related to crop growth simulations with DNDC are available as the key input information (User's Guide for the DNDC Model, <http://www.dndc.sr.unh.edu/model/GuideDNDC95.pdf>). To produce such representative phenological and physiological input parameters for DNDC, DSSAT has clear comparative advantage because the DSSAT model is designed for simulating very detailed crop-growing process, including phenological details. The central steps for enriching the parameter value set of rice cultivars in the DNDC model and to enable the smooth up-scaling runs of DNDC within each rice-cropping zone of China's rice growing region are as follows. (1) calibrating rice genetic coefficients at the nine agro-meteorological stations using the DSSAT model and its GLUE algorithms; (2) converting the newly calibrated genetic coefficients into the format of DNDC; (3) reclassifying the cropping zones based on the spatial relationship between observed cropping practices at the nine stations and the two-digit classification of the AEZ cropping zones, so that each rice cropping zone has only one set of DNDC parameter values; and (4) simulating CH₄ and N₂O emissions under different scenarios using the DNDC model with the calibrated values of crop cultivar parameters remaining stable in each of the reclassified cropping zones, under the historical climate conditions from 1981 to 2010.

(Figure 2 and Table 2 about here)

2.4.1 Scenarios configuration

In order to find one or more feasible management methods which can meet the dual goal of maintaining the current level of rice production and reducing GHG emissions from the current emission level, we set up 4 management scenarios and simulate rice growing and GHG emission processes for a single rice growing season under each scenario.

The first one is the "Traditional Management" (TM) scenario, in which the application of chemical fertilization follows the existing practice and irrigation follows the current continuous flooding, with the timing and intensity as recoded in the observation data of the nine study sites.

Excessive application of nitrogenous fertilizer has been widely recognized as an important source of excessive N₂O emission from rice paddy fields, as discussed in the

339 introduction. We define a threshold/balanced fertilizer amount which guarantees the best
340 attainable yield with the minimum amount of necessary fertilizer application, meaning that an
341 application amount smaller than this threshold will lead to yield reduction even under ideal
342 weather and water management conditions, and an application amount larger than this
343 threshold will not lead to an increase in yield. In order to find this threshold, the maximum
344 amount of the observed fertilizer application at each station was employed as the starting
345 point. Then we ran DNDC simulations stepwise and at each step we cut down this maximum
346 amount by 5% and check its impact on the best attainable yield. In this way we found the
347 ratio of the threshold/balanced fertilizer amount to the real maximum application amount at
348 each of the 9 stations. We call this ratio the ‘balanced fertilizer ratio’ (Table 2). Consistent
349 with the acknowledgement in the literature, excessive application is present in all nine
350 stations, being 5-35% higher than the requirement for supporting the best attainable yield.
351 While the SCCD and JXNC sites reported a moderate extent of excessive fertilizer
352 application, all other sites showed significant room for reducing fertilizer application amount.
353 The above search procedure leads to the establishment of the second scenario, which consists
354 of the balanced fertilizer application and continuous flooding irrigation method. We call it the
355 “Balanced Fertilizer” (BF) scenario.

356 With the development of new crop management and cultivar breeding technology,
357 increasing number of farmers are using the midseason field drying method to replace the
358 traditional basin irrigation method, which could mitigate CH₄ emission effectively. We name
359 this scenario “Midseason Drainage” (MD), in which the application of fertilizer is as the
360 observed, but irrigation management takes the midseason field drying method.

361 The forth scenario, we call it “Comprehensive Mitigation” (CM), combines the balanced
362 fertilizer application and the midseason field drying irrigation method. Because changes in
363 water management method will affect nitrification and denitrification processes, under the
364 MD and CM scenarios, the balanced fertilizer application amount at JXNC decreases from 90%
365 to 80% and at LNTT increases from 80% to 95% (Table 2, BFR-1 and BFR-2).

366

367 **2.4.2 Calibration of cultivar parameters and DNDC validation**

368 Key rice cultivar parameters related to the simulation of crop growth and GHG
369 emissions in DNDC include maximum biomass and C:N ratio of grain, leaf, stem and root,
370 respectively; optimum rice growing temperature; and the required accumulative degree days
371 (TDD) from sowing to maturity. In order to improve the information on rice cultivars in the
372 DNDC model, we first calculate the maximum grain biomass based on the yield records at

373 each observation site. We determine the best attainable yield based on the maximum value of
374 the multi-year yield components records, which includes the maximum grain number per
375 tiller and the corresponding grain weight, maximum tiller number per plant and the optimum
376 plant density. This way of determining the maximum grain biomass is in line with the
377 corresponding requirements in the DNDC setting. It also guarantees that the ways we find for
378 reducing CH₄ and N₂O emission are able to maintain the best attainable yield. Second, we
379 employ the GLUE module in the DSSAT model to calibrate the rice genetic coefficients by
380 targeting at the maximum grain biomass at each station. We used the outputs of DSSAT
381 model calibrated to calculate, for each site, the maximum biomass and the C:N ratio for each
382 part of the rice plant, and also the harvest index (HI). In the calculation of the C:N ratio, we
383 also take reference from the relevant information in the AEZ database to justify the range of
384 our calculations. Third, optimum temperature for rice growing is translated from reference
385 temperature in AEZ directly and the TDD is calculated based on the daily weather data during
386 each rice growing season over the period of 1981-2010. Table 3 reports the results of the
387 above calibration.

388
389 *(Tables 3-5 about here)*

390
391 We then ran the DNDC model using the newly calibrated cultivar parameter values
392 (Table 3), and validated the model by comparing the simulations against the observed best
393 attainable yield at the site level. The ideal field management practices are used to ensure that
394 the growing process is free from water and nitrogen stress, and only influenced by weather
395 and soil. We report both the ranges of simulated yields and the Relative Absolute Error
396 (RAE), as presented in Eq. (1), to evaluate the consistency between the observed and the
397 simulated values.

398
399
$$\text{RAE} = \frac{|\text{Obs} - \text{Simul}|}{\text{Obs}} \times 100\% , \quad (1)$$

400
401 where “obs” refers to the observed value and “simu” the result of DNDC model simulation at
402 the give site. Because the focus of DNDC is on the interactions between the C and N
403 biogeochemical cycles and the primary ecological drivers in the cropping process, rather than
404 on simulating the detailed crop growing process, the major phenology information such as
405 plating and maturity days are the input of DNDC. This means that the performance
406 evaluation of DNDC should be based on the comparison between observed and simulated
407 yield and emissions.

408 Table 4 reports the observed best attainable yield, the minimum, mean, and maximum of
409 the simulated yields, and the average RAE at the nine stations for the period of 1981-2010. It
410 shows that while at 6 of the 9 stations, the observed attainable yield lies within the
411 uncertainty range of the simulated yields, the observed yield at JLYJ is 119 kg higher (with an
412 average RAE at 4.69%) than the simulated maximum and that at SDLY and GDGZ is 313 kg
413 (average RAE 7.72%) and 290 kg (average RAE 8.13%) lower than the simulated minimum,
414 respectively. Given that the gap between the observed yield and the nearest border value of
415 the simulated yield is less than 5% at these 3 stations, we can accept that that the simulated
416 attainable yield matches the observed best attainable yield relatively well. This means that the
417 DNDC model with our enriched value set of cultivar parameters is able to simulate rice
418 production level with relatively good accuracy at each of the nine stations.

419 We do not directly test the DNDC simulations of CH₄ and N₂O emissions against the
420 corresponding field records because there is no observations on CH₄ and N₂O emissions at
421 the nine stations. Instead, we employed the experiment records at the Nanjing station
422 presented in Cai (1997) to validate the performance of the updated DNDC model. The same
423 experiment records were also used to validate the DNDC model by Cai et al. (2003) and
424 Fumuto et al. (2008). We ran DNDC using daily weather, soil and farming management data
425 from Cai et al. (2003) and Fumuto et al. (2008) for the same experimental site. For cultivar
426 parameters, we used the calibrated values at Zhengjiang station, which is 65 km to the east of
427 Nanjing, on the same Yangtze River bank area. Table 5 compares our results with those of Cai
428 et al. (2003) and Fumuto et al. (2008). Our simulated yield is 7782.5 kg ha⁻¹, which is 12%
429 higher than the observed yield. In contrast, there is no yield validation results in Cai et al.
430 (2003) and Fumuto et al. (2008). Our CH₄ emission result of 77 kg C ha⁻¹ is 1/3 higher than
431 the observed value but still 11 kg C ha⁻¹ lower than the result of Fumuto et al. (2008). Our
432 N₂O emission result of 0.5 kg N ha⁻¹ is much closer to the observed value than that of Cai et
433 al. (2003), which is 8 times higher than the observed value (Table 5).

434

435 **2.4.3 Reclassifying the rice cropping zones**

436 The cropping zone system defines the land use units in the AEZ by climate, soil and
437 terrain characteristics that are relevant to specific crop production. Cropping zones typically
438 represent the spatial distribution of crop cultivars in historical climate conditions (Tian et al.,
439 2012). In this research, the original two-digit rice cropping zone map of China as defined by
440 the AEZ model is employed. There are 14 rice cropping zones. For 9 of these 14 zones, we
441 directly established one-to-one correspondence between the zone and the station within the

442 zone. For each of the other 5 zones, the closest suitable cultivar station was chosen for the
443 zone. In this way, we reclassified the existing 14 zones into 9. The map of the reclassified rice
444 cropping zones, overlaid with the paddy field map of China in 2000, is presented in Figure 1.

445
446 *(Figures 3-7 about here)*

447 **3. RESULTS**

448 **3.1 The yield prediction performance of the original and updated DNDC models at the** 450 **regional level**

451 To show the improvement brought about by the cropping-zone specific enrichment of
452 rice cultivar parameters in terms of yield prediction at the regional level, we ran the DNDC
453 model with both the default and the enriched/updated value set of cultivar parameters across
454 paddy grid-cells for the best single season of rice. The two maps in Figures 3 show the results
455 on yield predictions from the DNDC model by using the default and enriched cultivar
456 parameter values, respectively. The predicted yields in both maps are presented as the
457 averages over 1981-2010. Figure 3-a shows that the single season rice yield is less than
458 4000kg ha⁻¹ in a very large part of the middle and lower reaches of the Yangtze River Basin,
459 which is much lower than observations in this most important rice producing region of China.
460 In sharp contrast, this undesirable gap does not show up in Figure 3-b. In terms of the
461 cropping zone average, the predicted yields in Figure 3-b range from 7000kg ha⁻¹ to 10000kg
462 ha⁻¹. These results validate our previous argument that using a single set of cultivar parameter
463 values cannot represent the richness of rice cultivars in a large rice producing country like
464 China and can result in poor prediction. This comparison confirms the necessity to calibrate
465 parameter values for more cultivars at multiple representative sites and to employ the
466 enriched parameter values to drive DNDC for the model applications over a large region.

467 468 **3.2. Site-level simulations**

469 The results of site-level simulations under the field management scenario of Traditional
470 Management (TM), Balanced Fertilizer (BF), Midseason Drainage (MD) and Comprehensive
471 Management (CM) are summarized into boxplots as presented in Figures 4 and 5. Figure 4
472 shows that these four field management methods are able to maintain the best attainable yield
473 under the condition without water and nitrogen stress. Formal *t*-tests also confirm this.

474 Figures 5-a and 5-b show the results on CH₄ and N₂O emissions, respectively. We first
475 focus on the comparison between TM and BF. The set of boxplots for CH₄ does not suggest

476 any significant change when moving from TM to BF. For example, at sites HNXYY, JXNC and
477 LNTT, the mean CH₄ emission decreased by less than 1% when adopting the balanced
478 fertilizer technique, whereas at other six stations, CH₄ emission barely increased, in the range
479 0.11%-4.25%. In contrast, the set of boxplots for N₂O shows significant mitigation of N₂O
480 emissions at all stations in relation to the balanced application technique, with reductions in
481 emissions that ranged 10%-69% and an average reduction across all sites of 33%.

482 Second we compare the results between TM and MD. Figures 5-a and 5-b show that
483 employing midseason drainage irrigation method mitigated CH₄ emission significantly, with
484 a reduction ratio ranging 18%-39% and an average reduction across all sites by 25%.
485 However, this new water management measure did not yield consistent results in terms of
486 changes in N₂O emissions. At sites JSZJ and JXNC, N₂O emissions in fact increased by 24%
487 and 20%, respectively, whereas at the other 7 stations, N₂O emissions decreased in the range
488 4%-32%.

489 The third comparison is between TM and CM. Figures 5-a and 5-b show significant
490 reductions in both CH₄ (18%-40%) and N₂O emissions (12%-60%). The mitigation impacts
491 of this management scenario outperformed the other scenarios at all nine stations, as a result
492 of positive interactions between the water and fertilizer management measures tested. We
493 further carried out formal *t*-tests to check the level of statistical significance of the differences
494 between TM and CM at each site. The *t*-test results indicate that the reduction of CH₄
495 emission is consistently significant at the 1% level across all sites, and the reduction of N₂O
496 is statistically significant at the 5% (at LNTT site) or 1% level (at other 7 sites), with the only
497 exception at JXNC.

498

499 **3.3 Regional-level simulations**

500 We extended the simulations of comprehensive mitigation (CM) scenario to the paddy
501 grid-cells in each of the 9 re-classified rice cropping zone to quantify the regional effect of
502 the comprehensive mitigation measure. Figure 6 shows the changes in the predicted yields
503 under the CM scenario versus TM scenario at the grid-cell level. It shows that the CM
504 measure resulted in yield increases in China's major rice producing regions – the Sichuan
505 Basin and the middle and lower reaches of the Yangtze River Basin; yield losses of 5%-10%
506 in parts of Northeast China, Ningxia's Hetao irrigation district and the northeast part of
507 Jiangsu province; and no changes or slight yield losses of less than 2% in other areas. At the
508 same time, the CM measure led to significant reductions in CH₄ and N₂O emissions (Figure
509 7), thus resulting in significant decreases in the GHG emission intensity (emissions per unit

510 product) of rice.

511 In terms of total annual CH₄ emissions from paddy fields under traditional water and
512 fertilizer management practices, DNDC simulated an annual mean value of 7892 Gg (1 Gg =
513 10⁹ g) C per year over 1981-2010. A nationwide switching from the traditional practice to the
514 comprehensive mitigation measure reduced CH₄ emissions by 1940 Gg C, or 25% in total,
515 and by 8% to 35% across most paddy grid-cells, as shown in Figure 7a. The reduction effect
516 was highly significant in the north part of Jiangxi province, large parts of Hunan and
517 Zhejiang provinces and the south part of Anhui province.

518 In terms of total annual N₂O emissions under traditional management practices, DNDC
519 simulated an annual mean value of 44 Gg N per year over 1981-2010. The nationwide switch
520 of water and management practice from TM to CM reduced N₂O emissions by 17 Gg N or 38%
521 in total, and by 10% to 75% across most paddy grid-cells as shown in Figure 7b. The most
522 significant mitigation effect was simulated in Northeast China, Jiangsu and Ningxia
523 provinces, while there no significant changes in emissions were simulated in Hubei province.

524

525 **4 DISCUSSION AND CONCLUSION**

526 Our site simulations suggest that comprehensive mitigation measures that combine
527 midseason drainage and balanced fertilizer applications can significantly reduce CH₄ and
528 N₂O emissions from paddy rice fields, without rice yield losses. This result is in line with
529 field experiment results from the Nanjing station presented by Cai et al. (1997). Our site
530 simulations for obtaining a balanced N fertilizer application ratio highlighted a 25%
531 excessive application rate in Zhenjiang station of Jiangsu province, very close to the 23.6%
532 estimate that resulted from the field experiments of Chen et al. (2016) and the 15-25%
533 estimate made by Hofmeier et al. (2015) in the same province.

534 Our aggregated results across all paddy fields in China show that mean annual total CH₄
535 emissions under prevalent traditional management practices is 7892 Gg C yr⁻¹ over the period
536 of 1981-2010, well within the range of 6000 to 12000 Gg C yr⁻¹ simulated by Li et al. (2005)
537 based on DNDC runs using county-level data, but still about double the levels estimated
538 under the IPCC Tier 1 methodology by FAOSTAT (FAOSTAT, 2016). In terms of average
539 CH₄ fluxes per hectare under traditional management practices, our result is 186 kg C ha⁻¹ yr⁻¹
540 for the period of 1981-2010, which is in the interval of 9 to 725 kg C ha⁻¹ yr⁻¹ indicated by a
541 field validation of the DNDC model in Cai et al. (2003) and the interval of 90 to 214 kg C ha⁻¹
542 yr⁻¹ produced by DNDC simulations at two sites in Liaoning and Jiangsu Provinces
543 (Frolking et al., 2004). Our results also show that the annual total N₂O emission from paddy

544 fields under traditional management practices is 43.9 Gg N yr⁻¹, which is close to the result of
545 35.7 Gg N as calculated for China's paddy fields as a whole by Gao et al. (2011), but
546 significantly lower than the simulation results of 290 to 410 Gg N yr⁻¹ as presented in Li et al.
547 (2005). In terms of average N₂O fluxes per hectare per year under the traditional management
548 practice, our result is 1.04 kg N ha⁻¹ yr⁻¹ during 1981-2010, which is located in the interval of
549 0.14 to 4.42 kg N ha⁻¹ yr⁻¹ as reported in Akiyama et al. (2005) based on the a summary of the
550 observed data.

551 The contribution of this research is not limited to confirming the existing assessments on
552 CH₄ and N₂O inventories. It aims to quantify, at both the site and regional levels, the extent to
553 which the major alternative water and fertilizer management methods can lead to significant
554 reduction of CH₄ and N₂O emissions without causing yield reduction. For this purpose, this
555 research enriches the value set of cultivar parameters of the DNDC model by effectively
556 communicating with the DSSAT-rice model and the AEZ model, and up-scales the DNDC
557 runs within each of the AEZ rice cropping zones.

558 More importantly, our systematic assessment focused on the effect of comprehensive
559 mitigation measures, which combines a balanced fertilizer application approach with the
560 midseason field drying method, and their evaluation against corresponding impacts on food
561 production potential. Our results show that switching from traditional fertilizer and water
562 management practices to comprehensive mitigation measures can lead to significant
563 reductions in both CH₄ and N₂O emissions. CH₄ emission can be reduced by 18-40% across
564 the nine representative stations, by 8-35% across almost all paddy grid-cells of China, and by
565 25% at the national level. N₂O emission can be reduced by 12-60% across the nine
566 representative sites, by 10-75% across a vast majority of grid-cells in China's paddy fields,
567 and by 38% at the national level. These findings indicate that there is significant room for
568 reducing GHG emissions in the Chinese rice producing sector. Measures such as midseason
569 drainage and balanced fertilization, based on crop requirements and soil testing, can achieve
570 the triple benefits of maintaining or even in some cases increasing production, while lowering
571 agricultural input costs and reducing GHG emissions. In future research, more mitigation
572 management methods, such as alternate wetting and drying water management for rice
573 (AWD), and returning straw and zero tillage, could be evaluated at both site and regional
574 scale, providing the necessary observation records become available for model calibration.

575 Several limitations characterize this study, some of them generically applicable to all
576 similar modeling exercises involving up-scaling in space from experimental field station
577 results. These include uncertainty in many of the assumptions used to distribute local weather,

578 soil and management parameters information over grid-cells. Two limitations are specific to
579 this study of paddy rice in China. First, only the most important single rice rotation was
580 considered, while double cropping rice was not studied. This may lead to biased estimation
581 because single cropping system typically require less N fertilizer, with weaker soil
582 denitrification reactions in cases where there is no additional crop and fertilizer inputs in the
583 fallow season. Future studies should investigate GHG emissions dynamics in double rice
584 cropping systems and other rotations with rice. Second, although the nine stations we chose
585 are representative at the two-digit cropping zone level, cultivar differences are present even
586 within individual two-digit cropping zones. The methodology presented in this research will
587 nonetheless be applicable to introduce more local rice cultivars into the DNDC model.

588

589 **References**

- 590 Abdalla, M., Kumar, S., Jones, M., Burke, J., Williams, M., 2011. Testing DNDC model for
591 simulating soil respiration and assessing the effects of climate change on the CO₂ gas flux from
592 Irish agriculture. *Global Planet. Change* 78, 106–115.
- 593 Akiyama, H., Yagi, K., Yan, X., 2005. Direct N₂O emissions from rice paddy fields: summary of
594 available data. *Global Biogeochem. Cycles* 19, GB1005.
- 595 Alley, R.B., Marotzke, J., Nordhaus, W.D., Overpeck, J.T., Peteet, D.M., Pielke, R.A., et al., 2003.
596 *Abrupt Climate Change*. *Science* 299, 2005-2010.
- 597 Batjes, N. H., 2009. Harmonized soil profile data for applications at global and continental scales:
598 updates to the WISE database. *Soil Use Manage.* 25, 124-127.
- 599 Beheydt, D., Boeckx, P., Sleutel, S., Li, C., van Cleemput, O., 2007. Validation of DNDC for 22 long-
600 term N₂O field emission measurements. *Atmos. Environ.* 41, 6196-6211.
- 601 Beven, K., Freer, J., 2001. Equifinality, data assimilation, and uncertainty estimation in mechanistic
602 modelling of complex environmental systems using the GLUE methodology. *J. Hydrol.* 249, 11-
603 29.
- 604 Blasone, R.S., Vrugt, J.A., Madsen, H., et al. 2008. Generalized likelihood uncertainty estimation
605 (GLUE) using adaptive Markov chain Monte Carlo sampling. *Adv Water Resour* 31(4): 630-648.
- 606 Cai, Z., Xing, G., Yan, X., Xu, H., Tsuruta, H., Yagi, K., Minami K., 1997. Methane and nitrous oxide
607 emissions from rice paddy fields as affected by nitrogen fertilizers and water management. *Plant
608 Soil* 196, 7-14.
- 609 Cai, Z., Sawamoto, T., Li, C., Kang, G., Boonjawat, J., Mosier, A., et al., 2003. Field validation of the
610 DNDC model for greenhouse gas emissions in East Asian cropping systems. *Global Biogeochem.
611 Cycles* 17 GB1107.
- 612 Challinor, A. J., Watson, J., Lobell, D. B., Howden, S. M., Smith, D. R., Chhetri, N. 2014. A meta-
613 analysis of crop yield under climate change and adaptation. *Nature Clim. Change* 4:287-291.
614 DOI: 10.1038/nclimate2153.
- 615 Chen, H., Yu, C., Li, C., Xin, Q., Huang, X., Zhang, J., et al., 2016. Modeling the impacts of water
616 and fertilizer management on the ecosystem service of rice rotated cropping systems in China.
617 *Agric. Ecosyst. Environ.* 219, 49-57.
- 618 Dong, H., Yao, Z., Zheng, X., Mei, B., Xie, B., Wang, R., et al., 2011. Effect of ammonium-based,
619 non-sulfate fertilizers on CH₄ emissions from a paddy field with a typical Chinese water
620 management regime. *Atmos. Environ.* 45, 1095-1101.
- 621 FAO, 2007. Mapping Biophysical Factors That Influence Agricultural Production and Rural
622 Vulnerability. Environment and Natural Resources Series 10. FAO, Rome, Italy.
- 623 FAO, 2016. Rice Market Monitor, April 2016. Trade and Markets Division, Food and Agriculture
624 Organization of the United Nations, Rome. Available at
625 http://www.fao.org/fileadmin/templates/est/COMM_MARKETS_MONITORING/Rice/Images/

626 [RMM/RMM_APR16.pdf](#).

627 FAO/IIASA/ISRIC/ISSCAS/JRC, 2009. Harmonized World Soil Database (version 1.1). FAO, Rome,
628 Italy and IIASA, Laxenburg, Austria.

629 FAOSTAT, 2016. Emissions-Agriculture Domain. <http://www.fao.org/faostat/en/#data/GR/visualize>

630 Fischer, G., Nachtergaele, F., Prieler, S., Teixeira, E., van Velthuisen, H.T., Tóth, G., et al., 2012.
631 Global Agro-Ecological Zones (GAEZ v3.0): Model Documentation. IIASA and FAO,
632 Laxenburg, Austria and Rome, Italy.

633 Fischer, G., Shah, M., Tubiello, F.N., van Velthuisen, H.T., 2005. Socioeconomic and climate change
634 impacts on agriculture: an integrated assessment, 1990–2080. *Philosophical Transactions of the*
635 *Royal Society B* 360, 2067–2073.

636 Frothing, S., Li, C., Braswell, R., Fuglestedt, J., 2004, Short- and long-term greenhouse gas and
637 radiative forcing impacts of changing water management in Asian rice paddies. *Glob. Chang. Bio.*
638 10, 1180-1196.

639 Fumoto, F., Kobayashi, K., Li, C., Yagi, K., and Hasegawa, T., 2008. Revising a process-based
640 biogeochemistry model (DNDC) to simulate methane emission from rice paddy fields under
641 various residue management and fertilizer regimes. *Glob. Change Biol.* 14, 382-402.

642 Gao, B., X. T. Ju, Q. Zhang, P. Christie, F. S. Zhang, 2011. New estimates of direct N₂O emissions
643 from Chinese croplands from 1980 to 2007 using localized emission factors. *Biogeosciences*, 8,
644 3011–3024.

645 Gao, M.F., Qiu, J.J., Li, C.S., Wang, L.G., Li, H., Gao, C.L., 2014. Modeling nitrogen loading from a
646 watershed consisting of cropland and livestock farms in China using Manure-DNDC. *Agr.*
647 *Ecosyst. Environ.* 185, 88–98.

648 Gijssman, A.J., Jagtap, S.S., Jones, J.W., 2002. Wading through a swamp of complete confusion: how
649 to choose a method for estimating soil water retention parameters for crop models. *European*
650 *Journal of Agronomy* 18, 75–105.

651 Gijssman, A.J., Thornton, P.K., Hoogenboom, G., 2007. Using the WISE database to parameterize soil
652 inputs for crop simulation models. *Computers and Electronics in Agriculture* 56, 85–100.

653 Gilhespy, S.L., Anthony, S., Cardenas, L., Chadwick, D., Pardo A., Li, C., et al., 2014. First 20 years
654 of DNDC (DeNitrification DeComposition): Model evolution. *Ecol. Model.* 292, 51-62.

655 Giltrap, D., Li, C., Saggart, S., 2010. DNDC: A process-based model of greenhouse gas fluxes from
656 agricultural soils. *Agr. Ecosyst. Environ.* 136, 292-300.

657 Gohari, A., Eslamian, S., Abedi-Koupaei, J., Bavani, A.M., Wang, D., Madani, K., 2013. Climate
658 change impacts on crop production in Iran's Zayandeh-Rud River Basin. *Science of the Total*
659 *Environment* 442, 405–419.

660 He, J., Jones, J., Graham, W., Dukes, M., 2010. Influence of likelihood function choice for estimating
661 crop model parameters using the generalized likelihood uncertainty estimation method. *Agr. Syst.*
662 103, 256-264.

663 Hofmeier, M., Roelcke, M., Han, Y., Lan, T., Bergmann, H., Böhm, D., et al., 2015. Nitrogen
664 management in a rice-wheat system in the Taihu Region: recommendations based on field
665 experiments and surveys. *Agric. Ecosyst. Environ.* 209, 60-73.

666 Hoogenboom G, Jones JW, Wilkens PW, et al. 2010. Decision Support System for Agro-technology
667 Transfer, Version 4.5, Volume 1: Overview. University of Hawaii, Honolulu, USA.

668 IPCC, 2006. IPCC Guidelines for National Greenhouse Gas Inventories, Inst. for Global Environ.
669 Strategies, Hayama, Japan.

670 IPCC, 2013. Climate Change 2013: The Physical Science Basis. Contribution of Working Group I to
671 the Fourth Assessment Report of the Intergovernmental Panel on Climate Change. Cambridge
672 Univ. Press. Cambridge.

673 IPCC, 2014. Climate Change 2014: Summary for Policymakers. Contribution of Working Group III to
674 the Fourth Assessment Report of the Intergovernmental Panel on Climate Change. Cambridge
675 Univ. Press. Cambridge.

676 Itoh, M., Sudo, S., Mori, S., Saito, H., Yoshida, T., Shiratori, Y., et al., 2011. Mitigation of methane
677 emissions from paddy fields by prolonging midseason drainage. *Agric. Ecosyst. Environ.* 141,
678 359-372.

679 Johnson-Beebout, E. S., Angeles, R. O., Alberto, R. M. C., Buresh, J. R., 2009. Simultaneous
680 minimization of nitrous oxide and methane emission from rice paddy soils is improbable due to
681 redox potential changes with depth in a greenhouse experiment without plants. *Geoderma.* 149,
682 45-53.

683 Jones, W. J., Antle, M. J., Basso, B., Boote, J. K., Conant, T. R., Foster, I., et al., 2016. Brief history of
684 agricultural systems modeling. *Agr Syst.* <http://dx.doi.org/10.1016/j.agsy.2016.05.014>)

685 Jones, J.W., Hoogenboom, G., Porter, C.H., Boote, K.J., Batchelor, W.D., Hunt, L.A., et al., 2003. The
686 DSSAT cropping system model. *Europ. J. Agronomy* 18, 235-265.

687 Karl, T.R., Trenberth, K.E., 2003. Modern Global Climate Change. *Science* 302, 1719-1723.

688 Lane, L. J., 1982. Distributed model for small semi-arid watersheds. 3. *Hydr. Div. Am. Soc. Civ. Eng.*
689 108, 1114-1131.

690 Li, C., 2000. Modeling trace gas emissions from agricultural ecosystems. *Nutr. Cycl. Agroecosys.* 58,
691 259-276.

692 Li, C., 2007. Quantifying greenhouse gas emissions from soils: scientific basis and modeling
693 approach. *Soil Sci. Plant Nutr.* 53, 344-352.

694 Li, C., Frolking, S., Harriss, R., 1994. Modeling carbon biogeochemistry in agricultural soils. *Global*
695 *Biogeochem. Cycles* 8, 237-254.

696 Li, C., Frolking, S., Frolking, T.A., 1992. A model of N₂O evolution from soil driven by rainfall
697 events: 1. Model structure and sensitivity. *J. Geophys. Res.* 97, 9759-9776.

698 Li, C., Frolking, S., Xiao, X., Moore, B., Boles, S., Qiu, J., et al., 2005. Modeling impacts of farming

699 management alternatives on CO₂, CH₄, and N₂O emissions: A case study for water management
700 of rice agriculture of China. *Global Biogeochem. Cycles* 19, GB3010.

701 Li, C., Salas, W., Zhang, R., Krauter, C., Rotz, A., and Mitloehner, F., 2012. Manure-DNDC: a
702 biogeochemical process model for quantifying greenhouse gas and ammonia emissions from
703 livestock manure systems. *Nutr. Cycl. Agroecos.* 93, 163-200, doi: 10.1007/s10705-012-9507-z,
704 2012.

705 Liu, J., Liu, M., Tian, H., Zhuang, D., Zhang, Z., Zhang, W., et al., 2005. Spatial and temporal patterns
706 of China's cropland during 1990–2000: an analysis based on Landsat TM data. *Remote Sensing*
707 *of Environment* 98, 442–456.

708 Masutomi, Y., Takahashi, K., Harasawa, H., Matsuoka, Y., 2009. Impact assessment of climate change
709 on rice production in Asia in comprehensive consideration of process/parameter uncertainty in
710 general circulation models. *Agriculture, Ecosystems and Environment* 131, 281–291.

711 McCuen, R.H., 2003. *Modeling Hydrologic Change: Statistical Methods*. Lewis Publishers, New York.

712 Miao, Y., Stewart, B.A., Zhang, F., 2010. Long-term experiments for sustainable nutrient management
713 in China. A review. *Agron. Sustain. Dev.* 31, 397-414.

714 Pathak, H., Li, C., Wassmann, R., 2005. Greenhouse gas emissions from Indian rice fields: calibration
715 and upscaling using the DNDC model. *Biogeosciences* 2, 113-123.

716 Penning de Vries, F., Teng, P., Metselaar, K., Hunt, L.A., 1992. *Designing Improved Plant Types: A*
717 *Breeder's Viewpoint, Systems Approaches for Agricultural Development*, vol. 2. Springer,
718 Netherlands, pp. 3–17.

719 Pohlert, T., 2004. Use of empirical global radiation models for maize growth simulation. *Agricultural*
720 *and Forest Meteorology* 126, 47–58.

721 Prasada Rao, G.S.L.H.V. 2008. *Agricultural Meteorology*, PHI Learning Pvt. Ltd., Delhi.

722 Ritchie, J.T., Godwin, D.C., Singh, U., 1989. Soil and Water inputs for IBSNAT crop models, In
723 *DSSAT, IBSNAT Symposium, Part I, Las Vegas, Nevada*.

724 Seidl, M., Batchelor, W., Fallick, J., Paz, J., 2001. GIS-crop model based decision support system to
725 evaluate corn and soybean prescriptions. *Appl. Eng. Agric.* 17, 721-728.

726 Smith, P., Trines, E., 2007. Agricultural measures for mitigating climate change: will the barriers
727 prevent any benefits to developing countries? *Int. J. Agric. Sust.* 4, 173-175.

728 Smith, P., 2012. Agricultural greenhouse gas mitigation potential globally, in Europe and in the UK:
729 what have we learnt in the last 20 years? *Glob. Chang. Biol.* 18, 35-43.

730 Tang, H.J., Qiu, J.J., Van Ranst, E., Li, C.S. 2006. Estimations of soil organic carbon storage in
731 cropland of China based on DNDC model. *Geoderma* 134, 200–206.

732 Thorp, K., DeJonge, K., Kaleita, A., Batchelor, W., Paz, J., 2008. Methodology for the use of DSSAT
733 models for precision agriculture decision support. *Comput. Electron. Agr.* 64, 276-285.

734 Tian, Z., Zhong, H., Shi R., Sun, L., Fischer, G., Liang, Z., 2012. Estimating potential yield of wheat
735 production in China based on cross-scale data-model fusion. *Front Earth Sci.* 6, 364-372.

736 Tian, Z., Zhong, H., Sun, L., Fischer, G., van Velthuis, H., Liang, Z. 2014. Improving performance
737 of Agro-Ecological Zone (AEZ) modeling by cross-scale model coupling: An application to
738 japonica riceproduction in Northeast China. *Ecological Modelling* 290, 155–164.

739 Tonitto, C., David, M.B., Drinkwater, L.E., Li, C.S., 2007. Application of the DNDC model to tile-
740 drained Illinois agroecosystems: model calibration, validation, and uncertainty analysis. *Nutr.*
741 *Cycl. Agroecosys.* 78, 51–63.

742 Tubiello, F.N., Fischer, G., 2007. Reducing climate change impacts on agriculture:global and regional
743 effects of mitigation, 2000–2080. *Technological Forecastingand Social Change* 74, 1030–1056.

744 Verburg, P.H., Chen, Y., Veldkamp, T., 2000. Spatial explorations of land use change and grain
745 production in China. *Agric. Ecosyst. Environ.* 82, 333-354.

746 Wang, G., Chen, S. 2012. A review on parameterization and uncertainty in modeling greenhouse gas
747 emissions from soil. *Geoderma* 170, 206–216.

748 Wang, L.G., Qiu, J.J., Tang, H.J., Li, H., Li, C.S., van Ranst, E. 2008. Modelling soil organic carbon
749 dynamics in the major agricultural regions of China. *Geoderma* 147, 47–55.

750 Wang, S., Huang, G.H., Huang, W., et al. 2015. A fractional factorial probabilistic collocation method
751 for uncertainty propagation of hydrologic model parameters in a reduced dimensional space. *J*
752 *Hydrol* 529: 1129–1146.

753 Wu, F., Zhang, H., Li, L., Chen, F., Huang, F., Xiao, X., 2008. Characteristics of CH₄ emission and
754 greenhouse effects in double paddy soil with conservation tillage. *Scientia Agricultura Sinica* 41,
755 2703-2709.

756 Yan, X., Akiyama, H., Yagi, K., Akimoto, H., 2009. Global estimations of the inventory and
757 mitigation potential of methane emissions from rice cultivation conducted using the 2006
758 Intergovernmental Panel on Climate Change Guidelines. *Global Biogeochem. Cycles* 23,
759 GB2002.

760 Zhang, L., Zhuang, Q., Li, X., Zhao, Q., Yu, D., Liu, Y., et al. 2016. Carbon sequestration in the
761 uplands of Eastern China: An analysis with high-resolution model simulations. *Soil & Tillage*
762 *Research* 158, 165–176.

763 Zhang, Y., Li, C., Trettin, C. C., Li, H., and Sun, G., 2002. An integrated model of soil, hydrology and
764 vegetation for carbon dynamics in wetland ecosystems, *Global Biogeochem. Cy.* 16, 1061, doi:
765 10.1029/2001GB001838.

766

767

768 Table 1. Information of the nine representative observation stations

Site	Location	Soil texture	Mean daily temperature range (°C)	Precipitation range (mm)	Mean precipitation (mm)
AHHF	31.87°N 117.23°E	Loam	24.2-27.3	228.4-1064.2	578.6
HNXY	32.12°N 114.08°E	Silty-clay	24.2-27	151.7-1161.4	677.0
JLYJ	42.88°N 129.47°E	Clay-loam	15.2-18.4	331.7-790.0	467.4
JSZJ	32.18°N 119.47°E	Clay-loam	25-27.1	269.8-1327.0	669.1
JXNC	28.55°N 115.95°E	Clay-loam	23-25.6	501.4-1341.2	820.2
LNTT	41.42°N 123.32°E	Sandy-clay-loam	19-22.3	354.1-916.3	569.5
SCCD	30.7°N 103.83°E	Clay-loam	22-24.1	488.1-1050.2	733.8
SDLY	35.05°N 118.35°E	Clay-loam	22.5-24.9	441.8-1106.7	715.6
GDGZ	23.05°N 113.47°E	Clay-loam	18.9-25.8	570.1-1640.7	1012.5

769 Notes: The statistics on temperature and precipitation is for the single rice growing season over the period of
770 1981-2010.

771

772

773

774

775 Table 2. Observed level of fertilizer application and the balanced fertilizer ratio (BFR) at the
776 nine stations

Site	AHHF	HNXY	JLYJ	JSZJ	JXNC	LNTT	SCCD	SDLY	GDGZ
Fertilizer App (kgN ha ⁻¹)	335.0	255.3	330.5	273.0	334.5	203.6	252.9	186.0	250.0
BFR-1 (%)	85	80	65	75	90	80	95	70	65
BFR-2 (%)	85	80	65	75	80	95	95	70	65

777 Notes: BFR-1 refers to the BFR under continues flooding scenario and BFR-2 under the midseason drainage and
778 comprehensive management scenarios.

779

780

781

782

783 Table 3. Calibrated values of cultivar parameters for DNDC at the nine representative sites

Site	GB	HI	GF	LF	SF	RF	ND	OT	TDD
AHHF	11436.33	0.5273	0.448	0.201	0.201	0.15	209.588	27	3859.00
HNNY	11597.39	0.5179	0.440	0.205	0.205	0.15	215.382	25	3776.00
JLYJ	10761.25	0.5311	0.452	0.199	0.199	0.15	168.919	22	2965.00
JSZJ	11539.50	0.5078	0.432	0.209	0.209	0.15	217.479	25	3884.30
JXNC	9055.58	0.6058	0.514	0.168	0.168	0.15	150.094	30	2594.95
SCCD	9883.21	0.5644	0.480	0.185	0.185	0.15	172.349	25	3873.80
SDLY	9900.00	0.4958	0.422	0.214	0.214	0.15	158.480	25	3808.60
LNTT	9528.57	0.5521	0.470	0.190	0.190	0.15	146.662	22	3471.55
GDGZ	7801.40	0.5486	0.466	0.192	0.192	0.15	138.883	30	3351.45

784 Notes: GB denotes grain biomass (kg/ha/yr), HI harvest index, GF grain-fraction, LF leaf-fraction, SF stem-
785 fraction, RF root-fraction, ND N demand (kgN/ha/yr), OT optimum temperature (°C), TDD accumulative
786 degree days from emergence to maturity (°C).

787

788

789

790

791 Table 4. The observed best attainable yield, the minimum, mean, and maximum of the
792 simulated yields, and the average RAE at the nine stations (1981-2010)

Site	Observed yield (kg)	Simulated attainable yield (kg)			Average RAE (%)
		Minimum	mean	maximum	
AHHF	10,815	8,869	10,266	10,952	5.086
HNNY	10,024	9,141	10,125	10,992	0.998
JLYJ	10,500	9,249	10,009	10,381	4.686
JSZJ	10,140	8,891	10,494	10,852	3.491
JXNC	8,812	8,268	8,623	8,892	2.156
SCCD	9,240	8,861	9,240	9,531	0.000
SDLY	8,580	8,893	9,242	9,582	7.716
LNTT	9,184	8,276	8,752	9,195	4.704
GDGZ	6,945	7,235	7,511	7,677	8.135

793

794

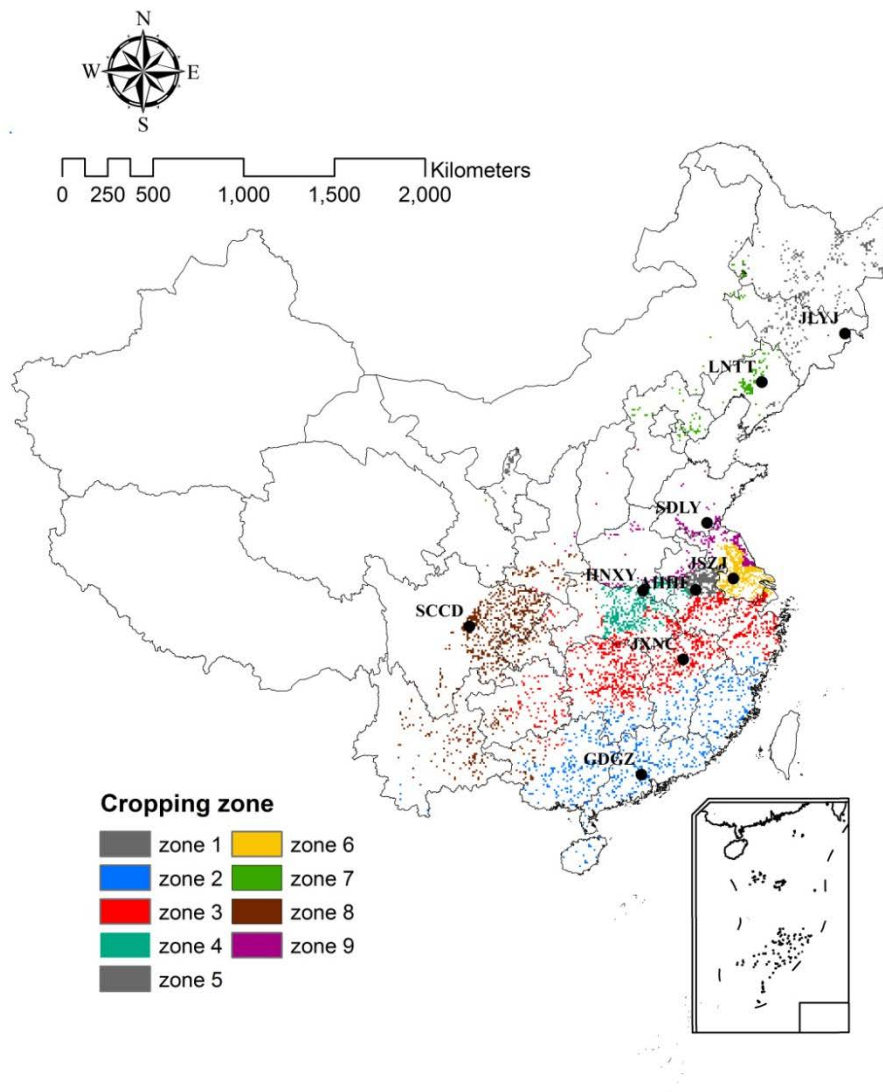
795

796 Table 5. Rice yield, CH₄ and N₂O emissions at the Nanjing site in 1994.

	Observed (Cai et al., 2003)	Simulated with DNDC		
		<i>Our results</i>	<i>Cai et al. (2003)</i>	<i>Fumuto et al. (2008)</i>
Yield (kg ha ⁻¹)	6918.8	7782.5		
CH ₄ (kg C ha ⁻¹)	57.8	77	47.1	88
N ₂ O (kg N ha ⁻¹)	0.62	0.5	5.70	

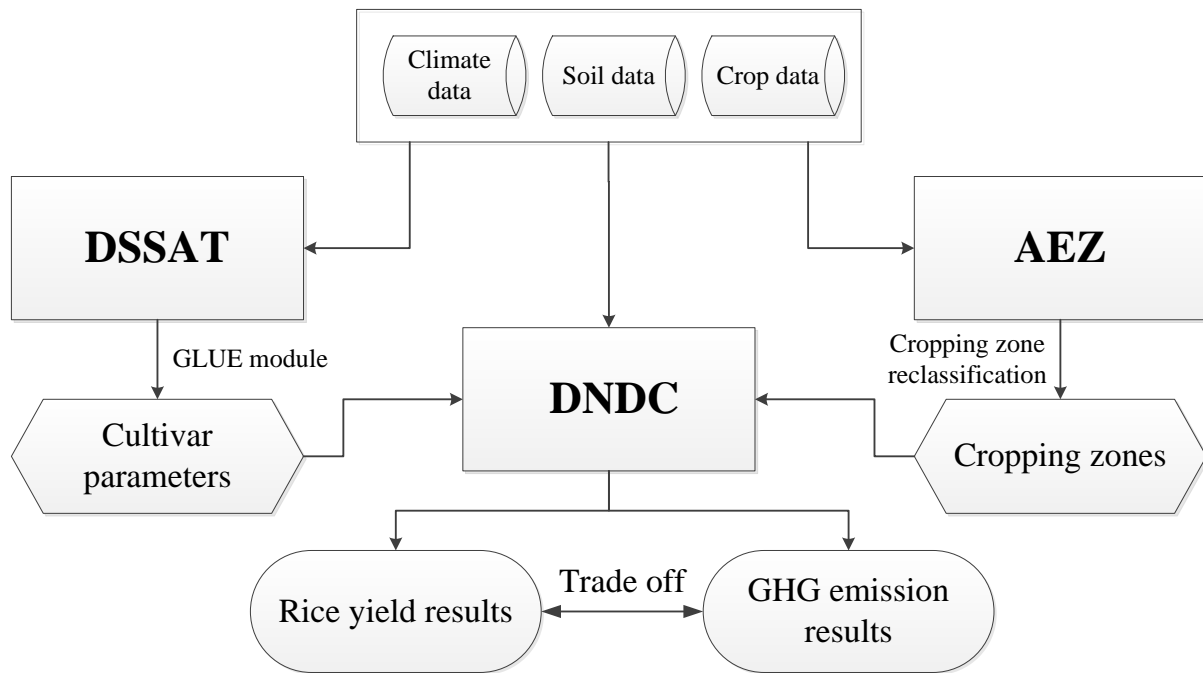
797 Note: Observation records and simulation results are for the same single rice growing season in 1994.

798



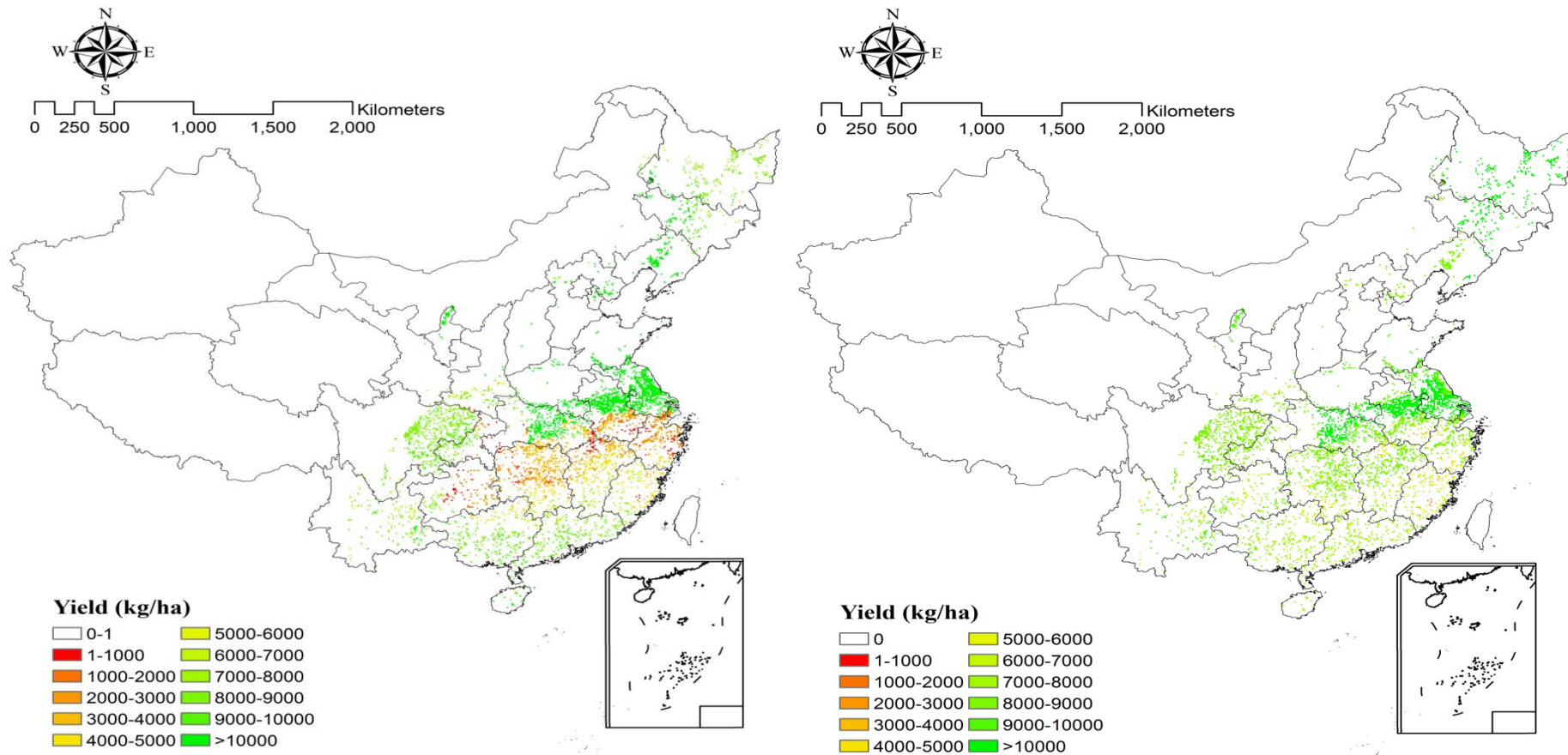
799
 800
 801
 802
 803
 804
 805
 806
 807
 808

Figure 1. The reclassified rice cropping zone map of China based on 9 observation stations. Color scheme distinguishes the 9 zones and big black dots stand for the observation stations



809
 810
 811
 812
 813
 814

Figure 2. Flowchart of the model coupling procedure



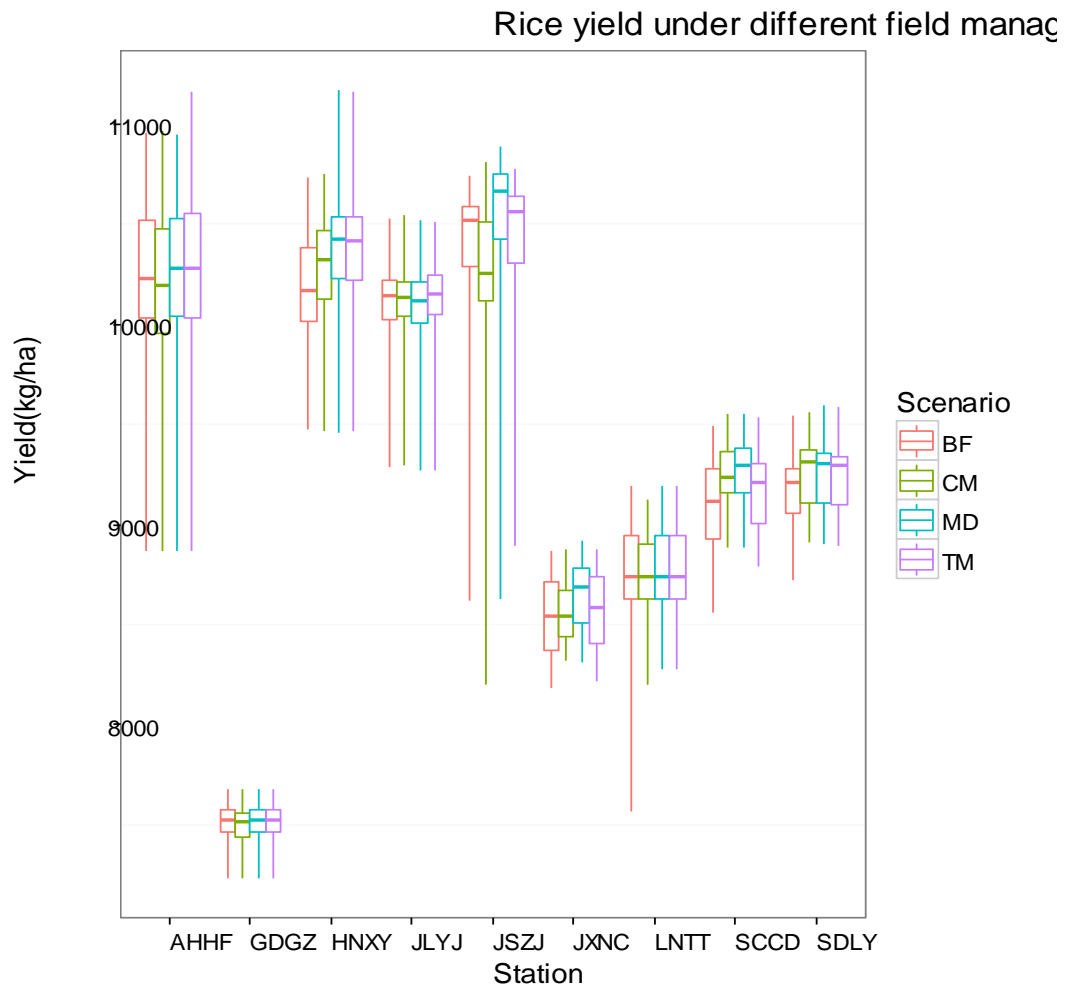
815
816

817 Figure 3. The grid-cell results of rice yield simulation from the original DNDC (left, denoted as Figure 3-a) and coupled DNDC (right, Figure 3-
818 b) model, average over 1981-2010

819

820

821



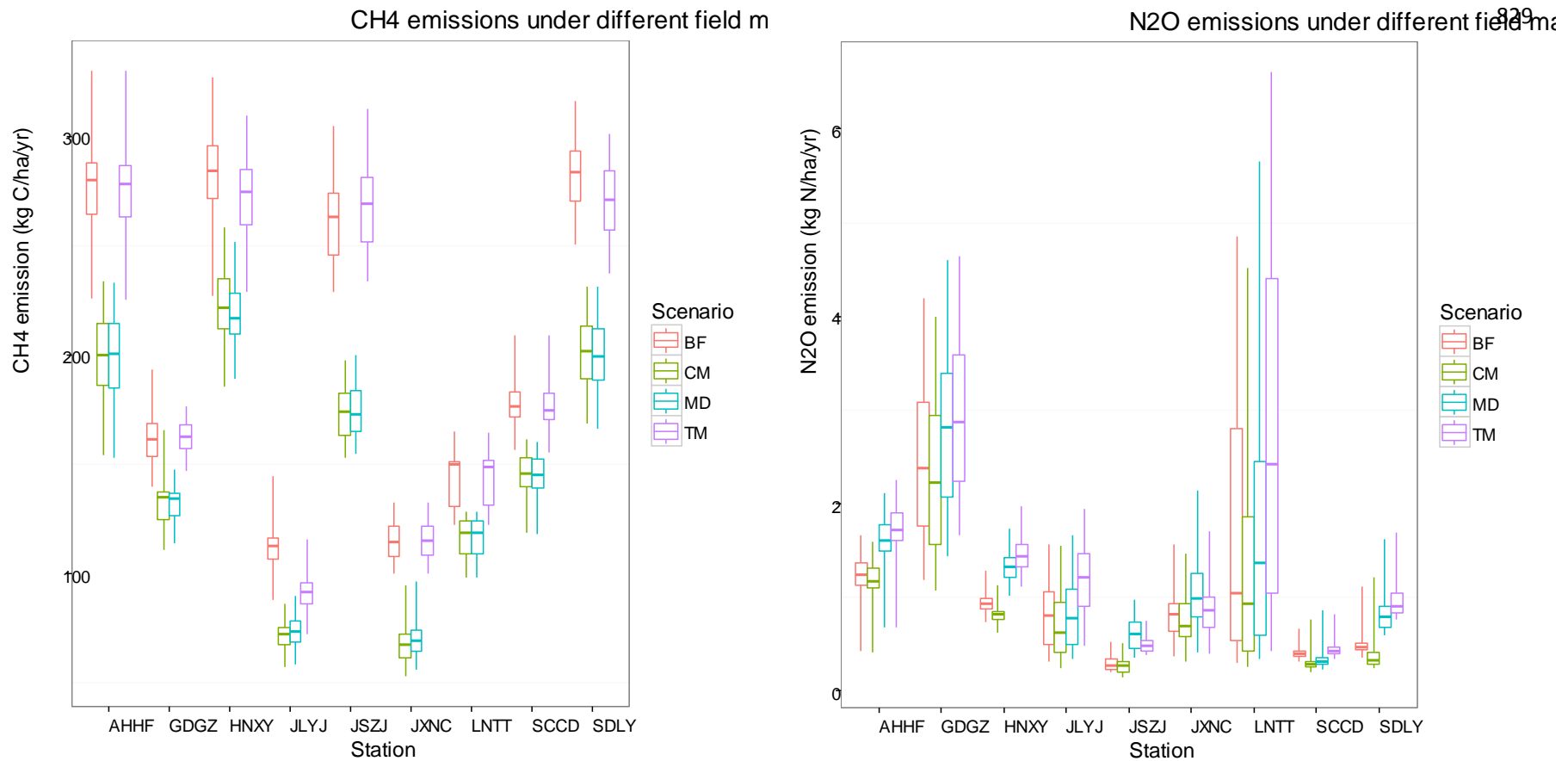
822

823 Figure 4. The boxplots of rice yields under field management scenarios of Traditional
824 Management (TM), Balanced Fertilizer (BF), Midseason Drainage (MD) and Comprehensive
825 Management (CM).

826

827

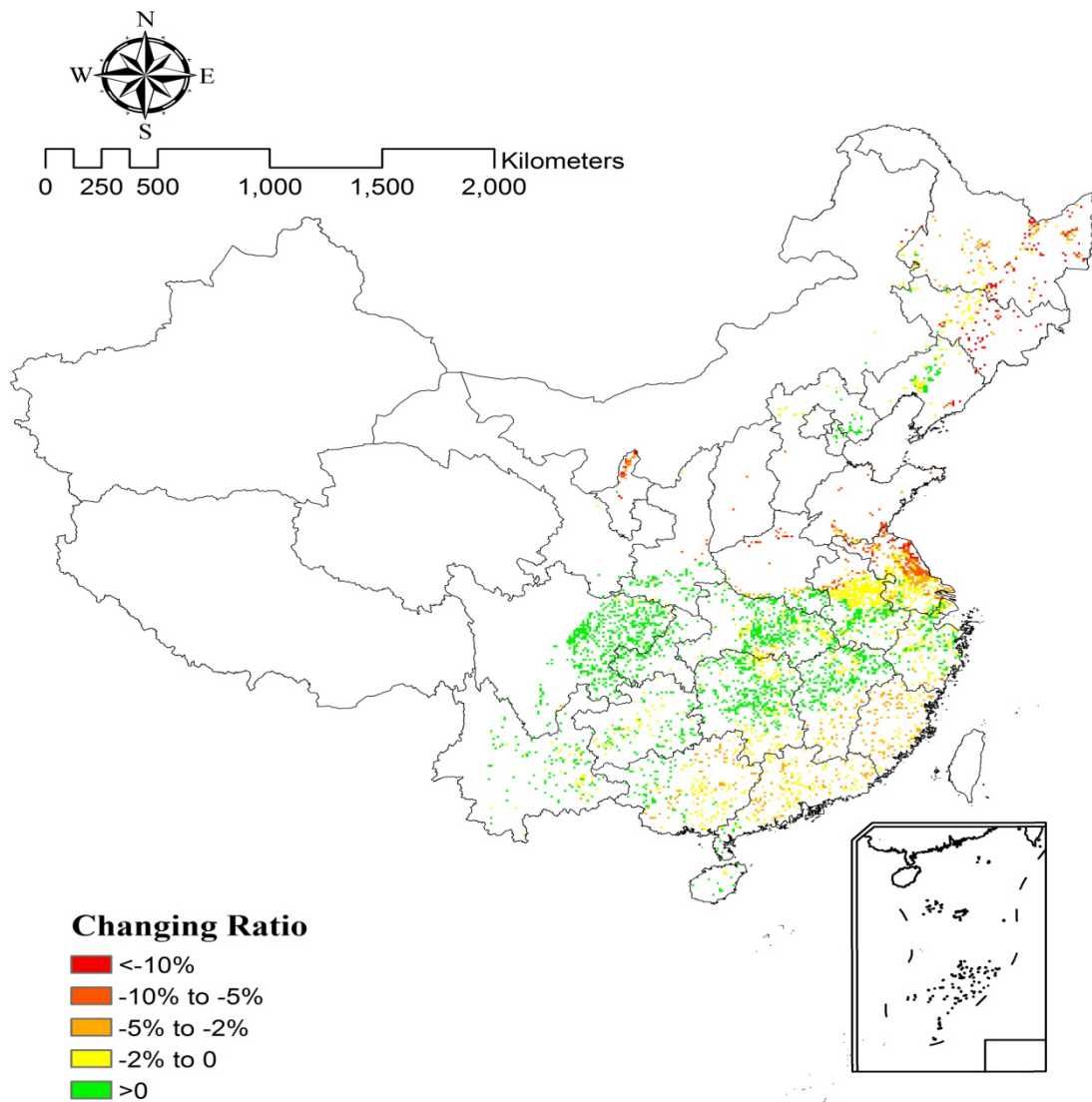
828



830 Figure 5. The boxplots of methane emission (left, denoted as Figure 5-a.) and nitrous oxide emission (right, Figure 5-b.) under field management
831 scenarios of Traditional Management (TM), Balanced Fertilizer (BF), Midseason Drainage (MD) and Comprehensive Management (CM).

832

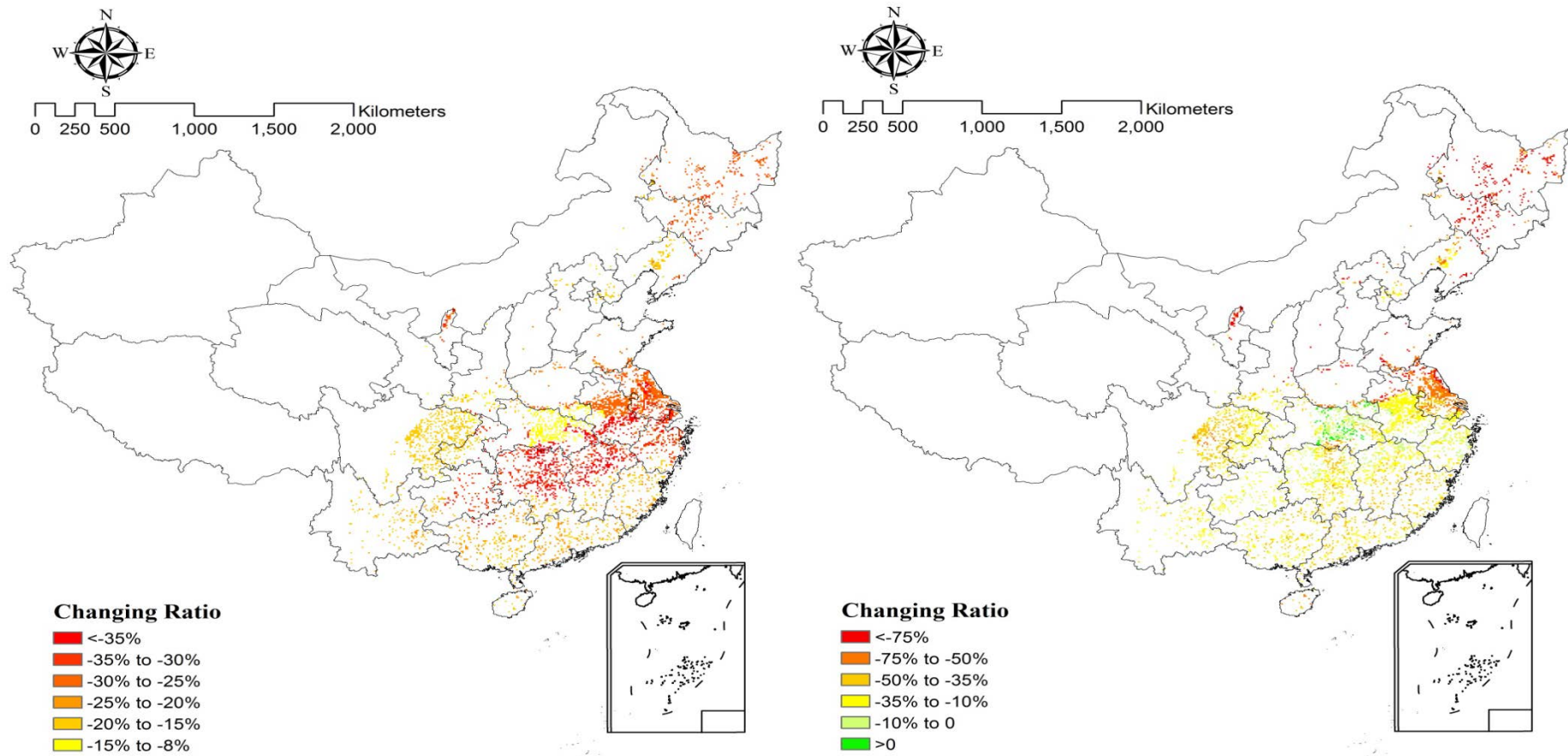
833



834

835 Figure 6. Changes of the simulated best attainable yields at the grid-cell level under the
836 comprehensive mitigation scenario versus the traditional management scenario

837



838

839 Figure 7. Changes in CH₄ emission (left, denoted as Figure 7-a.) and N₂O emission (right, Figure 7-b.) at the grid-cell level under the
840 comprehensive mitigation scenario versus traditional management scenario